

Autocorrelations from fluctuation scale dependence by inversion

T. A. Trainor, R. J. Porter and D. J. Prindle

(Dated: December 24, 2018)

Fluctuations in nuclear collisions can be measured as a function of momentum-space binning scale over a scale interval bounded by detector two-track resolution and acceptance. Fluctuation scale dependence is related to two-particle correlations by a Fredholm integral equation. That equation can be inverted by standard numerical methods to yield an autocorrelation distribution on difference variables as a projection of the full two-particle distribution which retains most of the correlation information in a more compact form. Autocorrelation distributions are typically more easily interpreted in terms of physical mechanisms than fluctuation measurements.

PACS numbers: 24.60.Ky, 25.75.Gz

Keywords: fluctuations, autocorrelations, inverse problem, heavy ions, relativistic nuclear collisions

I. INTRODUCTION

Nuclear collisions are studied in large part *via* the correlation structure of the hadronic final state [1]. The large-scale correlation structure of pair density $\rho(\vec{p}_1, \vec{p}_2)$ on a two-particle momentum space can provide qualitatively new information about collision dynamics compared to single-particle density $\rho(\vec{p})$ studied with conventional inclusive measures. Since the full two-particle momentum space cannot be visualized, it is necessary to project onto one or more subspaces, retaining as much of the correlation structure as possible. For relativistic nuclear collisions the *autocorrelation* distribution represents a nearly lossless projection [2] of the two-particle momentum distribution onto a visualizable subspace.

Measurements of nonstatistical fluctuations of multiplicity n and event-wise mean transverse momentum $\langle p_t \rangle$ have been proposed to study the QGP in heavy ion collisions [3, 4, 5, 6, 7]. Direct interpretation of fluctuation measurements is often difficult. However, the bin-size or *scale* dependence of fluctuations is determined by the correlation structure of the underlying distribution [8, 9]. We have found that fluctuation scale dependence can be inverted by a numerical procedure to obtain autocorrelation projections.

In this paper we derive an exact relationship between fluctuation scale dependence and autocorrelation distributions on *difference variables* in the form of an integral equation. We describe the procedure required to invert the integral equation [10] and thereby obtain autocorrelations from the fluctuation scale dependence. We apply that procedure to Monte Carlo simulations and examine the precision of the autocorrelations which result. We find that the resulting autocorrelations are typically directly interpretable in terms of physical mechanisms.

II. AUTOCORRELATIONS

An autocorrelation is the projection of a two-particle distribution onto its difference variables, *e.g.*, a distri-

bution on (x_1, x_2) projected onto $x_1 - x_2$, a lossless strategy if correlations are invariant on sum variable $x_1 + x_2$. Autocorrelations are well-established in time-series analysis [11]. They also appear in various aspects of nuclear collision analysis. A series of correlation measurements on rapidity in elementary collisions e^+e^- , p - p and p - \bar{p} [12] was critical to formulating the phenomenological representation of nonperturbative QCD contained in the Lund model [13]. To accommodate limited statistics the two-particle distribution on rapidity was typically divided into two regions by conditions placed on the rapidity of one (test or tagged) particle. The joint distribution for particles of opposite ‘charge’ was then projected onto the rapidity of a second particle. Those conditional projections approximate an autocorrelation distribution. Direct determination of *joint* autocorrelations on momentum subspace (η, ϕ) has been extensively implemented in multiparticle correlation analysis of fixed-target p-p experiments [14]. Such joint autocorrelations also provide unbiased access to jet correlations. HBT analysis of quantum correlations in nuclear collisions also employs autocorrelations on momentum difference variables [15].

The examples above involve *direct* determination of autocorrelations by pair counting. Alternatively, autocorrelations can be obtained by inverting the bin-size or scale dependence of fluctuations. Inversion of fluctuation scale dependence to obtain autocorrelations provides three advantages: 1) direct determination of an autocorrelation by pair ratios is $O(n^2)$, whereas a fluctuation calculation is $O(n)$, thereby reducing computation time; 2) autocorrelations obtained directly from pair ratios may have an arbitrary offset due to pair normalization ambiguities; and 3) as noted, fluctuations are less easily interpreted than autocorrelations in terms of physical mechanisms.

III. SUMMARY OF METHOD

We first summarize the basic elements of the *inverse problem* connecting fluctuations to correlations in nuclear collisions and introduce the final result: the inte-

gral equation between fluctuation scale dependence and two-particle correlations in the form of autocorrelation distributions.

Spaces and measures Momentum in a relativistic nuclear collision can be expressed as $\vec{p} \rightarrow (p_t, \eta, \phi)$, where p_t is transverse momentum relative to the collision axis, η is pseudorapidity and ϕ is momentum azimuth angle. Each momentum component x , bounded by acceptance Δx , can define a two-particle space (x_1, x_2) . Spaces x are partitioned into 1D *microbins* of fixed size ϵ_x limited below by detector resolution and *macrobins* with variable size or scale $\epsilon_x \leq \delta x \leq \Delta x$. Variation of macrobin contents and their moments with scale is the basis of fluctuation analysis.

Measure w (scalar p_t sum or particle sum n in the bin) is distributed on x . Transverse momentum p_t in a relativistic collision plays the dual role of a momentum-space component and of a thermodynamic quantity distributed on complementary momentum subspace (η, ϕ) . We refer to single-particle measure density $\rho(w; x)$ and histogram bin contents $\bar{w}_a \simeq \epsilon_x \rho(w; x_a)$, or two-particle density $\rho(w; x_1, x_2)$ and histogram $\overline{w_a w_b} \simeq \epsilon_x^2 \rho(w; x_a, x_b)$.

Correlation structure is defined by comparison of object and reference distributions. Reference distributions are constructed by averaging, formation of mixed pairs from different but similar collisions or by model functions. The reference distribution determines what correlations are retained by a differential correlation measure. For object distribution ρ_{obj} and reference distribution ρ_{ref} the difference density $\Delta\rho \equiv \rho_{obj} - \rho_{ref}$ represents the desired correlation structure, and $\Delta w \equiv w_{obj} - w_{ref}$ represents the corresponding difference histogram.

Fluctuations Fluctuations represent the correlation structure of binned distributions. In a nuclear collision a distribution total weight W (*e.g.*, total transverse momentum P_t or multiplicity N) falls within a detector acceptance $(\Delta\eta, \Delta\phi)$ divided into M macrobins of size $(\delta\eta, \delta\phi)$. Each macrobin (represented by single scale δx for brevity) contains in each event some integrated $w(\delta x)$ as a random variable. The conventional per-bin variance is $\sigma_w^2(\delta x) \equiv \overline{\{w(\delta x) - \bar{w}(\delta x)\}^2}$, where the overlines represent averages over all macrobins of size δx in all events of an ensemble [9]. The corresponding scale-dependent *per-particle* variance is defined by $\sigma_{w/}^2(\delta x) \equiv \sigma_w^2(\delta x)/\bar{n}(\delta x)$. Its small-scale limit $\sigma_{\bar{w}}^2$ is inclusive single-particle p_t variance $\sigma_{\bar{p}_t}^2$ if $w = p_t$, and is defined to be 1 (Poisson limit) if $w = n$. The scale-dependent *variance difference* defined by $\Delta\sigma_{w/}^2(\delta x) \equiv \sigma_{w/}^2(\delta x) - \sigma_{\bar{w}}^2$ is a definite integral of two-particle correlations over a scale interval [8].

Autocorrelations Autocorrelation A is the projection by averaging of a two-particle distribution onto difference variables. For relativistic nuclear collisions the 2D *joint* autocorrelation on $(\eta_\Delta, \phi_\Delta)$ is a nearly lossless projection from the 4D $(\eta_1, \eta_2, \phi_1, \phi_2)$ pair-momentum

space. We distinguish between autocorrelation histograms A and autocorrelation densities $\rho(x_\Delta)$. We define histogram difference $\Delta A \equiv A_{obj} - A_{ref}$ and corresponding density difference $\Delta\rho = \rho_{obj} - \rho_{ref}$.

Integral equation We seek an exact relation between fluctuation scale dependence and autocorrelations such that measurement of the former can be inverted to obtain the latter. Variation of $\Delta\sigma_{w/}^2$ on bin scales $(\delta\eta, \delta\phi)$ is represented by an *integral equation* which can be inverted to obtain an autocorrelation on difference variables $(\eta_\Delta, \phi_\Delta)$

$$\begin{aligned} \Delta\sigma_{w/}^2(m \epsilon_\eta, n \epsilon_\phi) &\equiv 2\sigma_{\bar{w}} \Delta\sigma_{w/}(m \epsilon_\eta, n \epsilon_\phi) \\ &= 4 \sum_{k,l=1}^{m,n} \epsilon_\eta \epsilon_\phi K_{mn;kl} \frac{\Delta\rho(w; k \epsilon_\eta, l \epsilon_\phi)}{\sqrt{\rho_{ref}(n; k \epsilon_\eta, l \epsilon_\phi)}}, \end{aligned} \quad (1)$$

which also defines *difference factor* $\Delta\sigma_{w/}$. Derivation of that integral equation and the techniques required for its inversion are the main subjects of this paper.

IV. FLUCTUATION SCALE DEPENDENCE

Variance as a fluctuation measure compares an object distribution to a reference composed of averages of the object distribution. The scale (bin size) dependence of fluctuations as measured by a variance is equivalent to a running integral of two-particle correlations. The difference between fluctuations across a scale interval is equivalent to a definite integral of correlations over that scale interval.

Measures and binnings The single-particle density $\rho(w; x)$ of measure w is distributed on bounded 1D space $x \in [-\Delta x/2, \Delta x/2]$, *i.e.*, within ‘acceptance’ Δx . The space is partitioned into equal macrobins of size δx referred to as the binning *scale*. The contents of bin s is $w_s \approx \delta x \rho(w, x_s)$. For a comparison of object and reference distribution we define difference histogram $\Delta w(\delta x) \equiv w_{obj}(\delta x) - w_{ref}(\delta x)$.

Variations We define the scale-dependent *total variance* of difference histogram $\Delta w(\delta x)$ by

$$\sigma_w^2(\Delta x, \delta x) \equiv \overline{\sum_{s=1}^{M(\Delta x, \delta x)} \{\Delta w_s(\delta x)\}^2}, \quad (2)$$

where s is a macrobin index, $M(\Delta x, \delta x)$ is the event-wise number of *occupied* macrobins of size δx in acceptance Δx , and the bar denotes an average over all events. This quantity is also a bin-based estimate of the *correlation integral* $C_2(w; \Delta x, \delta x)$ [16]. Because the total variance is extensive with respect to detector acceptance Δx we define several intensive forms which result in, respectively,

per-bin and per-particle variances and a total-variance density on x

$$\begin{aligned}\Sigma_w^2(\Delta x, \delta x)/M(\Delta x, \delta x) &\equiv \sigma_w^2(\delta x) & (3) \\ \Sigma_w^2(\Delta x, \delta x)/\bar{N}(\Delta x) &\equiv \frac{(\Delta w)^2}{\bar{n}} \\ &\equiv \sigma_{w/}^2(\delta x) \\ \Sigma_w^2(\Delta x, \delta x)/\Delta x &\simeq d\bar{n}/dx \sigma_{w/}^2(\delta x).\end{aligned}$$

Those factorized forms separate acceptance Δx and scale δx dependencies. The optimum choice among them depends on the physical source(s) of nontrivial fluctuations.

Variance differences In the small-scale limit where the particle occupancy of all *occupied* bins is 1 we have $\Sigma_w^2(\Delta x, \delta x \ll \Delta x) \rightarrow \bar{N}(\Delta x) \sigma_w^2$, the inclusive single-particle variance of w . For *central limit conditions* (independent w samples from a fixed parent distribution) the total variance is scale invariant: $\Sigma_w^2(\Delta x, \delta x) \equiv \bar{N}(\Delta x) \sigma_w^2$ over any scale interval for which CLT conditions are valid. The scale invariance of total variance is an alternative statement of the central limit theorem [8]. Deviations of $\Sigma_w^2(\Delta x, \delta x)$ from CLT invariance indicate the presence of w correlations. That connection leads to the definition of a fluctuation measure which is differential across a scale interval: the *total-variance difference*

$$\Delta \Sigma_w^2(\delta x_1, \delta x_2) \equiv \Sigma_w^2(\delta x_2) - \Sigma_w^2(\delta x_1), \quad (4)$$

which is zero if CLT conditions apply over the scale interval. The total variance difference for $\delta x_2 = \delta x$ and $\delta x_1 \ll \Delta x$ is given by

$$\begin{aligned}\Delta \Sigma_w^2(\Delta x, \delta x) &= \bar{N}(\Delta x) \left\{ \sigma_{w/}^2(\delta x) - \sigma_w^2 \right\} \\ &\equiv \bar{N}(\Delta x) \Delta \sigma_{w/}^2(\delta x), & (5)\end{aligned}$$

which defines *per-particle* variance difference $\Delta \sigma_{w/}^2$. The variance difference across a scale interval is a measure of correlations in $\rho(w; x)$ integrated over that scale interval; it is equivalent to the integral of a difference autocorrelation across the same scale interval, as described below. From that equivalence we obtain the integral equation relating autocorrelations to fluctuation scale dependence.

V. AUTOCORRELATION DEFINITIONS

The autocorrelation of a two-particle distribution on binned space (x_1, x_2) consists of averages over diagonal regions of the 2D space which then occupy single bins of the autocorrelation histogram on the difference variable. We describe the construction of autocorrelations from a two-particle distribution by two direct (that is, not by fluctuation inversion) methods.

Two-particle spaces In Fig. 1, two-particle density $\rho(w; x_1, x_2)$ is distributed on space (x_1, x_2) . In that

space it is useful to define *sum and difference variables* $x_\Sigma \equiv x_1 + x_2$ and $x_\Delta \equiv x_1 - x_2$. Distance along those variables is measured on x as shown in Fig. 1 to avoid factors $\sqrt{2}$. If the correlation structure of single-particle density $\rho(w; x)$ is independent of mean position on x or *stationary* (equivalently, $\rho(w; x_1, x_2) \rightarrow \rho(w; x_\Sigma, x_\Delta)$ is independent of sum variable x_Σ) the corresponding auto-correlation density on x_Δ represents a lossless projection (all structure retained) of the two-particle density onto a lower-dimensional space: $\rho(w; x_\Sigma, x_\Delta) \rightarrow \rho(w; x_\Delta)$. For relativistic nuclear collisions that symmetry is nominally exact on ϕ (assuming ideal detection) and approximate on η or y_z (depending on the validity of ‘boost invariance’ over a specific y_z interval for a given collision system).

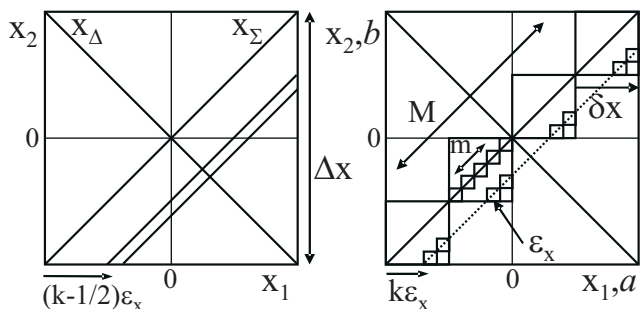


FIG. 1: Integration schemes for direct construction of auto-correlations: 1) normalized strip integrals (left panel) and 2) diagonal bin averages (right panel). Macrobins have variable size δx , microbins have fixed size ϵ_x . Bins on difference variable x_Δ are indexed by integer k .

Autocorrelation histograms Autocorrelation histograms can be constructed by three methods: 1) more directly by sorting particle pairs into 1D bins on momentum difference variables x_Δ as normalized strip integrals (Fig. 1, left panel), 2) less directly as weighted averages of diagonal combinations of microbins from a 2D histogram on space (x_1, x_2) (Fig. 1, right panel), 3) indirectly by *inverting* the scale dependence of a moment, variance or variance difference.

We introduce for the numerical integration microbins of fixed size ϵ_x such that there are m_δ microbins in a macrobin of variable size ($\epsilon_x \leq \delta x \leq \Delta x$) and m_Δ microbins in a fixed acceptance of size Δx . If difference variable x_Δ is partitioned into microbins indexed by k , two autocorrelation types, which depend on binning strategy on the difference variable, can be defined for an *aperiodic* distribution on x . Those autocorrelation types correspond to the two direct construction methods described above and illustrated in Fig. 1 (left and right panels respectively): 1) square bin edge on zero (strip integral – particle pairs indexed by i, j falling within the k^{th} x_Δ bin), then

$$A_k^{(1)}(w) \equiv \frac{1}{m_\Delta - |k| + 1/2} \overline{\sum_{ij=1}^N (w_i w_j)_{ij \in k}}, \quad (6)$$

with $|k| \in [1, m_\Delta]$ (w_i, w_j are single-particle values); and 2) triangular bin centered on zero (averages of 2D microbin contents indexed by a, b), then

$$A_k^{(2)}(w) \equiv \frac{1}{m_\Delta - |k|} \sum_{a=1}^{m_\Delta - |k|} \overline{w_a w_{a+k}}, \quad (7)$$

with $|k| \in [0, m_\Delta - 1]$ (average over all bins on diagonal bin array within acceptance, Fig. 1 (right panel) with $\delta x \rightarrow \Delta x$). Overlines indicate averages over all events. For a distribution *periodic* on x the type-1 autocorrelation is given by $A_k^{(1)}(w) \equiv 1/m_\Delta \sum_{ij=1}^N \overline{(w_i w_j)_{ij \in k}}$, with particles of any pair i, j falling within one period on x (the period then defines Δx). Binning strategies and indexing on x_Δ for the two cases are shown in Fig. 2. For autocorrelations constructed from a particle list (most efficient) the square bin index applies. For prebinned 2D space (x_1, x_2) the triangular bin index applies. For fluctuation inversion leading to autocorrelations either method may be used, but the rectangular bin index facilitates direct comparison between fluctuation inversion and the more efficient direct method 1) of autocorrelation construction.

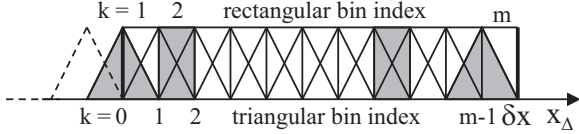


FIG. 2: Binning schemes on difference variable x_Δ : 1) square bins on x_Δ (Fig. 1 left panel) with $|k| \in [1, m]$, and 2) triangular projections of 2D bins (Fig. 1 right panel) with $|k| \in [0, m - 1]$.

Difference autocorrelations $\Delta A_k = A_{k,obj} - A_{k,ref}$ represents a subset of the correlation content of an *object* distribution. The type-1 number n reference autocorrelation obtained with mixed pairs (particles selected from different but similar events) is $A_{k,ref}^{(1)}(n) \equiv 1/(m_\Delta - |k| + 1/2) \overline{\sum_{ij \in k}} \equiv \bar{n}_k^2$ (i, j are particle indices). The type-2 equivalent based on bin averages is $A_{k,ref}^{(2)}(n) \equiv 1/(m_\Delta - |k|) \sum_{a=1}^{m_\Delta - |k|} \bar{n}_a \bar{n}_{a+k} \equiv \bar{n}_k^2$. The type-1 *difference* autocorrelation for measure w is defined in terms of sibling (same-event) and mixed pairs as $\Delta A_k^{(1)}(w) \equiv 1/(m_\Delta - |k| + 1/2) \overline{\sum_{ij \in k} \Delta w_i \Delta w_j}$. That form is illustrated in Fig. 1 (left panel). We can utilize bin averages $w_{a,ref} \equiv \bar{w}_a$ to define type-2 difference autocorrelation $\Delta A_k^{(2)}(w) \equiv 1/(m_\Delta - |k|) \sum_{a=1}^{m_\Delta - |k|} \overline{\Delta w_a \Delta w_{a+k}}$. As defined, $\Delta A_k^{(2)}(w)$ is a projection by averaging onto its difference variable of binned two-particle *covariance* distribution $\overline{\Delta w_a \Delta w_b}$ on (x_1, x_2) (a, b are microbin indices). That form is illustrated in Fig. 1 (right panel), with $\delta x \rightarrow \Delta x$). The difference autocorrelation, being a projection of $\Delta \rho(x_1, x_2)$ onto its difference variable, is

also a covariance distribution (most obvious for the type-2 formulation above), except for the $k = 0$ bin which is a variance at the microbin scale. Figs. 3 (right panels) and 5 show examples of difference autocorrelations obtained from fluctuation inversion.

VI. THE INTEGRAL EQUATION

We next obtain an exact correspondence between the per-particle variance and a type-2 difference autocorrelation. We use the relation between binning schemes in Fig. 2 to express per-particle variance as the scale integral of a type-1 difference autocorrelation, most efficiently obtained from a direct autocorrelation analysis. We then generalize to 2D momentum subspace (η, ϕ) to obtain the required integral equation relating fluctuation scale dependence on $(\delta\eta, \delta\phi)$ to joint autocorrelations on axial difference variables $(\eta_\Delta, \phi_\Delta)$.

Variations and type-2 autocorrelations Starting with the definition of total variance we obtain the exact relation of the per-particle variance to a weighted sum of type-2 autocorrelation elements. The total variance as a sum over occupied macrobins is given in Eq. (2). Since $\Delta w_s(\delta x) = \sum_{a \in s} \Delta w_a(\epsilon_x)$, the corresponding per-particle variance can be written as a sum over 2D microbins

$$\sigma_{w_f}^2(\delta x) = \frac{1}{\bar{n}(\delta x)} \sum_{k=1-m_\delta}^{m_\delta-1} \overline{\sum_{a,b=1 \dots m_\delta}^{b=a+k} \Delta w_a \Delta w_b}, \quad (8)$$

where the sums over indices a, b include only microbins within macrobins at scale δx , as in Fig. 1 (right panel), and the upper overline indicates an average over all occupied macrobins in the acceptance. Rearranging and noting that $\bar{n}(\delta x) \equiv m_\delta \bar{n}(\epsilon_x)$ we obtain

$$\sigma_{w_f}^2(\delta x = m_\delta \epsilon_x) = \sum_{k=1-m_\delta}^{m_\delta-1} \frac{m_\delta - |k|}{m_\delta} \times \left\{ \frac{\bar{n}_k(\epsilon_x)}{\bar{n}(\epsilon_x)} \left[\frac{1}{m_\delta - |k|} \sum_{a,b}^{b=a+k} \frac{\sqrt{\bar{n}_a \bar{n}_b}}{\bar{n}_k(\epsilon_x)} \left(\frac{\overline{\Delta w_a \Delta w_b}}{\sqrt{\bar{n}_a \bar{n}_b}} \right) \right] \right\} \quad (9)$$

where $\bar{n}_k(\epsilon_x) \equiv 1/(m_\delta - |k|) \overline{\sum_{a,b}^{b=a+k} \sqrt{\bar{n}_a \bar{n}_b}}$ is a geometric mean over microbins within macrobins at scale δx , and the upper overline denotes an average over all macrobins in the acceptance.

The quantities in parentheses are two-particle difference-histogram elements equivalent to density ratio $\epsilon_x \{ \Delta \rho(w) / \sqrt{\rho_{ref}(n)} \}_{ab}$. That 2D histogram represent *per particle* correlations in measure w on space (x_1, x_2) . The quantity in square brackets is a weighted average of those histogram elements over the k^{th} diagonal which *estimates* type-2 difference autocorrelation $\Delta \hat{A}_k^{(2)}(w) / \sqrt{\hat{A}_{k,ref}^{(2)}(n)}$, the per-particle autocorrelation

distribution on x_Δ . The quantity in curly brackets estimates autocorrelation elements $\Delta A_k^{(2)}(w)/\sqrt{A_{k,ref}^{(2)}(n)}$ which would be inferred from inversion of fluctuation scale dependence (*cf* Eq. (11)). If quantity \bar{n}_k varies significantly (possible on η_Δ , depending on collision system, detector acceptance and required precision) the $O(1)$ multiplicity-ratio factor \bar{n}_k/\bar{n} may be removed as a systematic correction to obtain the hatted autocorrelation in square brackets. This per-particle relation offers an optimized match between two-particle correlations and fluctuation measures.

Variance differences and type-1 autocorrelations We now transition from type-2 to type-1 autocorrelations in order to relate fluctuation scale dependence to the more efficient direct method of obtaining autocorrelations. The quantity in curly brackets in Eq. (9) estimates the type-2 difference autocorrelation defined previously as an average over *all* microbins on the k^{th} diagonal within the acceptance (Fig. 1, right panel, $\delta x \rightarrow \Delta x$). We rewrite Eq. (9), replacing the quantity in curly brackets by the difference autocorrelation which it estimates. We then re-express the variance difference in terms of an equivalent expression for the type-1 difference autocorrelation

$$\begin{aligned} \sigma_{w/\delta}^2(m_\delta \epsilon_x) &= \sum_{k=1}^{m_\delta-1} \frac{m_\delta - |k|}{m_\delta} \left\{ \frac{\Delta A_k(w)}{\sqrt{A_{k,ref}(n)}} \right\}^{(2)} \quad (10) \\ &= 2 \sum_{k=1}^{m_\delta} \frac{m_\delta - k + 1/2}{m_\delta} \left\{ \frac{\Delta A_k(w)}{\sqrt{A_{k,ref}(n)}} \right\}^{(1)} \\ &= 2 \sum_{k=1}^{m_\delta} \frac{m_\delta - k + 1/2}{m_\delta} \times \\ &\quad \times \left\{ \frac{\bar{n}_k(\epsilon_x)}{\bar{n}(\epsilon_x)} \left[\frac{1}{m_\Delta - k + 1/2} \sum_{i,j \in k}^N \frac{\overline{\Delta w_i \Delta w_j}}{\bar{n}_k(\epsilon_x)} \right] \right\}, \end{aligned}$$

where $\Delta w_i = w_i - \hat{w}$ for particle i , \hat{w} is the inclusive mean of w , $\bar{n}_k^2(\epsilon_x) \equiv \sum_{i,j \in k}^N 1/(m_\Delta - k + 1/2)$ for mixed pairs, and the quantity in square bracket is the autocorrelation obtained by direct method (1). Either expression (1) or (2) above can be used to define the integral equation relating fluctuation scale dependence to difference autocorrelations. The two forms correspond to the two binning schemes on the difference variable shown in Fig. 2.

Inclusive variance σ_w^2 in variance difference $\Delta \sigma_{w/\delta}^2(\delta x)$ corresponds to self pairs in the pair sums of Eq. (10). If those pairs are excluded from two-particle pair distributions and the autocorrelation definitions then the relations above apply to the variance *difference*, rather than the scale-dependent variance. For the type-1 autocorrelation we then obtain the integral equation

$$\Delta \sigma_{w/\delta}^2(m \epsilon_x) = 2 \sum_{k=1}^m K_{m;k} \frac{\Delta A_k(w; \epsilon_x)}{\sqrt{A_{k,ref}(n; \epsilon_x)}}, \quad (11)$$

where $K_{m;k} \equiv (m - k + 1/2)/m$ is an integration kernel representing the macrobin scheme, and we have dropped the subscript δ from index m . Autocorrelation difference density $\Delta \rho$ is related to the autocorrelation difference histogram by $\Delta A_k(w; \epsilon_x) \equiv \epsilon_x^2 \Delta \rho(w; k \epsilon_x)$. Likewise, $A_{k,ref}(n; \epsilon_x) \equiv \epsilon_x^2 \rho_{ref}(n; k \epsilon_x)$. The integral equation is then re-expressed in terms of a density ratio as

$$\Delta \sigma_{w/\delta}^2(m \epsilon_x) = 2 \sum_{k=1}^m \epsilon_x K_{m;k} \frac{\Delta \rho(w; k \epsilon_x)}{\sqrt{\rho_{ref}(n; k \epsilon_x)}}. \quad (12)$$

2D integral equation For a 2D scaling analysis on (η, ϕ) we generalize $\delta x \rightarrow (\delta \eta, \delta \phi)$ to obtain the per-particle w variance difference (also defining difference factor $\Delta \sigma_{w/\delta}$ [9]) as a 2D discrete integral equation

$$\begin{aligned} \Delta \sigma_{w/\delta}^2(m \epsilon_\eta, n \epsilon_\phi) &\equiv 2 \sigma_{\hat{w}} \Delta \sigma_{w/\delta}(m \epsilon_\eta, n \epsilon_\phi) \quad (13) \\ &= 4 \sum_{k,l=1}^{m,n} \epsilon_\eta \epsilon_\phi K_{mn;kl} \frac{\Delta \rho(w; k \epsilon_\eta, l \epsilon_\phi)}{\sqrt{\rho_{ref}(n; k \epsilon_\eta, l \epsilon_\phi)}}, \end{aligned}$$

with kernel $K_{mn;kl} \equiv (m - k + 1/2)/m \cdot (n - l + 1/2)/n$ representing the 2D macrobin system. This is a Fredholm integral equation which can be inverted to obtain autocorrelation density ratio $\Delta \rho_{kl}/\sqrt{\rho_{ref,kl}}$ as a per-particle correlation measure on difference variables $(\eta_\Delta, \phi_\Delta)$ from fluctuation scale dependence of $\Delta \sigma_{w/\delta}^2(\delta \eta, \delta \phi)$.

VII. THE INVERSE PROBLEM

We have established the relationship between a variance difference and the integral of an autocorrelation. Given the former as experimental data we wish to infer the latter as conveying the underlying physics in a more interpretable form. Joint (2D) autocorrelation distributions on difference variables $(\eta_\Delta, \phi_\Delta)$ are inferred from fluctuation scale dependence on $(\delta \eta, \delta \phi)$ by inverting those distributions according to Eq. (13) (those autocorrelation distributions are by construction symmetric about the origin on $(\eta_\Delta, \phi_\Delta)$). In standard nomenclature the variance difference on the left in Eq. (13) is ‘data’ \mathbf{D} and the autocorrelation density ratio on the right is ‘image’ \mathbf{I} . Schematically, $\mathbf{D} = \mathbf{T} \mathbf{I} \leftrightarrow \Delta \sigma_{w/\delta}^2 = \mathbf{K} \Delta \rho / \sqrt{\bar{\rho}}$.

Extracting the image Inverting an integral equation from data to image is usually nontrivial and has engendered a large literature [10]. Integration and inversion are mappings (matrix transformations \mathbf{T} , \mathbf{T}^{-1}) from one vector space to another. Forward integration from image to data can be represented by $\mathbf{D} = \mathbf{T} \mathbf{I} + \mathbf{N}$, (\mathbf{N} represents noise added to the data as part of measurement) with formal inverse $\mathbf{I}' = \mathbf{T}^{-1} \mathbf{D} = \mathbf{I} + \mathbf{T}^{-1} \mathbf{N}$, where \mathbf{I} is the true image. The image produced by naive mapping $\mathbf{I}' = \mathbf{T}^{-1} \mathbf{D}$ is typically dominated by small-wavelength components of image noise $\mathbf{T}^{-1} \mathbf{N}$, since \mathbf{T}^{-1} is a form of

differentiation (acting as a ‘high-pass’ filter). A smoothing procedure called *regularization* is used to reduce image noise while minimizing distortion of the true image.

Regularization By *smoothing* the inverted image $\mathbf{I}'_\alpha = \mathbf{T}_\alpha^{-1} \mathbf{D}$ with a regularization procedure (smoothing parameter α is defined below) we control the impact on the image of the statistical noise on the data. We treat each bin of the image as a free fitting parameter, but add a smoothing term with Lagrange multiplier α to the fit χ^2 to obtain $\chi_\alpha^2 \equiv \|\mathbf{D} - \mathbf{T} \mathbf{I}'_\alpha\|^2 + \alpha \|\mathbf{L} \mathbf{I}'_\alpha\|^2$. The first term measures the deviation of the integrated image from the data. The second term, with linear operator \mathbf{L} , measures the small-wavelength λ structure of the image. The optimum choice of α maximally reduces small- λ noise on \mathbf{I}'_α without significantly distorting the signal - the meaningful structure on true image distribution \mathbf{I} . Operator \mathbf{L} can take various forms [17]. The underlying assumption of a regularization procedure is that the statistical ‘noise’ is sufficiently distinct from the true correlation ‘signal’ on wavelength λ that operator \mathbf{L} , a measure of small- λ structure on \mathbf{I}'_α , can distinguish the two. We eliminate most of the small- λ noise while retaining as much large- λ signal as possible. As α increases, more small- λ noise is eliminated. At some point increasing α reduces the signal. By comparing the two elements of χ_α^2 as in Fig. 4 (left panel), the optimum value of α can be determined.

Statistical and systematic errors The autocorrelation (image) error distribution has two components: statistical error which survives smoothing and systematic error due to image distortion by smoothing. The optimum value of α should adequately reduce statistical noise relative to signal while minimally distorting the signal. The residual statistical noise and the signal distortion then depend on the optimum value of α . The linear relation between statistical errors on data and image is similar to that for data and image themselves. It is straightforward to invert that relation (using the optimized α value) to obtain mean-square errors $\delta^2 \mathbf{I}'_\alpha$ for the image histogram. Because of the structure of difference autocorrelation density ratio $\Delta\rho/\sqrt{\rho_{ref}}$ those errors tend to be uniform on the difference-variable space, making their characterization simple.

To estimate smoothing distortions, inferred image \mathbf{I}'_α can be integrated forward to become a new data distribution, and then inverted again to obtain a twice-smoothed image. That procedure is represented schematically by 1) $\mathbf{I}'_\alpha = \mathbf{T}_\alpha^{-1} \mathbf{D}$ (smoothed image from data inversion), 2) $\mathbf{D}_\alpha = \mathbf{T} \mathbf{I}'_\alpha$ (forward-integrated smoothed image), 3) $\mathbf{I}'_{\alpha\alpha} = \mathbf{T}_\alpha^{-1} \mathbf{D}_\alpha$ (twice-smoothed image). By comparing image distributions \mathbf{I}'_α and $\mathbf{I}'_{\alpha\alpha}$, assuming that the smoothing process is linear, one can estimate the smoothing distortions, usually largest at points of maximum gradient on the image. The smoothing error can then be displayed as a histogram or summarized as a fractional error of peaked structure on the image distribution.

VIII. MONTE CARLO EXAMPLES

We illustrate the determination of fluctuation scale dependence and inversion to autocorrelations with Monte Carlo data. The method described above is applied to data obtained from two Monte Carlo simulations of nuclear collisions: Hijing, which simulates A-A collisions, and Pythia, which simulates p-p collisions.

Hijing Au-Au 200 GeV p_t correlations Event generator Hijing-1.37 [18] was used to produce a total of 1M minimum-bias Monte Carlo collision events of two types: 1) *quench-off* Hijing – jet production enabled but no jet quenching and 2) *default* or *quench-on* Hijing – jet production and jet quenching both enabled. Each event type was then split into six centrality classes consisting of roughly equal fractions of total cross section. A more complete analysis of Hijing fluctuation data and inversion to p_t autocorrelations is described in [19]. For the fluctuation analysis charged particles with pseudorapidity $|\eta| < 1$, transverse momentum $p_t \in [0.15, 2]$ GeV/c and full azimuth were accepted.

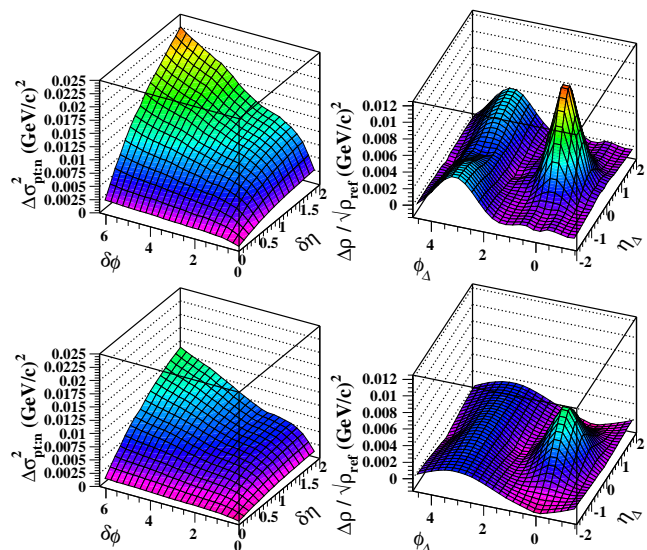


FIG. 3: Left panels: $\Delta\sigma_{p_t:n}^2$ (GeV/c)² distributions on binning scales ($\delta\eta, \delta\phi$) for central 0-15% collisions and two Hijing states: quench off (top panel) and quench on (bottom panel). Right panels: Corresponding autocorrelations on difference variables (η_Δ, ϕ_Δ).

Fig. 3 shows fluctuation scale dependence and corresponding autocorrelations for 0-15% central collisions and two Hijing configurations: quench-off (top panels) and quench-on (bottom panels). In the left panels are variance differences $\Delta\sigma_{p_t:n}^2(\delta\eta, \delta\phi)$ (GeV/c)². Whereas the physical interpretation of such fluctuation distributions is typically ambiguous, interpretation of the corresponding autocorrelations is often straightforward and gives access to critical parameters of physical phenomena, in this case the peak amplitude and widths. Au-

tocorrelation distributions on $(\eta_\Delta, \phi_\Delta)$ shown in Fig. 3 (right panels) contain two features: a same-side component ($|\phi_\Delta| < \pi/2$) and an away-side component ($\pi/2 < |\phi_\Delta| < \pi$). The dominant same-side peak can be identified with *minimum-bias* parton fragments (minijets): no high- p_t trigger condition is imposed in the analysis.

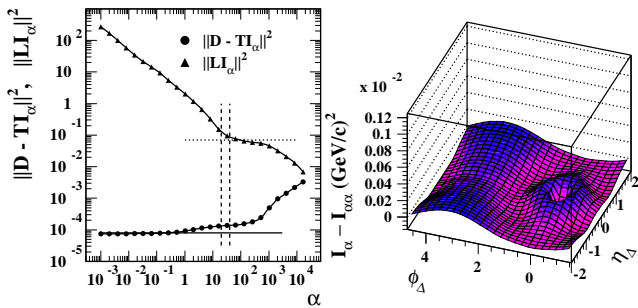


FIG. 4: Left panel: Distribution of $\|\mathbf{D} - \mathbf{TI}_\alpha\|^2$ (dots) and $\|\mathbf{LI}_\alpha\|^2$ (triangles) vs α for the 0-15% central quench-off data in Fig. 3 (upper-right panel). Deviation of $\|\mathbf{D} - \mathbf{TI}_\alpha\|^2$ from the extrapolation (horizontal solid line) indicates systematic error due to image smoothing. The vertical dashed lines bracket the optimal choice of α . Right panel: Distribution of estimated smoothing error $\mathbf{I}_\alpha - \mathbf{I}_{\alpha\alpha}$ on $(\eta_\Delta, \phi_\Delta)$, also for the 0-15% central quench-off autocorrelation in Fig. 3 (upper-right panel). Note the $10\times$ scale reduction compared to Fig. 3.

An illustration of α optimization is given in Fig. 4. Distributions $\|\mathbf{D} - \mathbf{TI}_\alpha\|^2$ and $\|\mathbf{LI}_\alpha\|^2$ on α shown in Fig. 4 (left panel) can be used to determine the optimum α value. The $\|\mathbf{D} - \mathbf{TI}_\alpha\|^2$ distribution is nearly constant at smaller α , indicating no loss of valid structure by smoothing. The $\|\mathbf{LI}_\alpha\|^2$ distribution falls rapidly, indicating substantial noise reduction. At some value of α $\|\mathbf{D} - \mathbf{TI}_\alpha\|^2$ begins to rise from the constant (extrapolated by the solid line), the deviation representing information loss from the image. Beyond that point there is a tradeoff between smoothing distortion and noise reduction. In the example of Fig. 4 the noise exhibits a stationary point at the same position (upper dotted line). The optimum choice of α is in the region bracketed by the vertical dashed lines.

Autocorrelation errors have two components: statistical errors derived from corresponding errors in fluctuation data, and distortion errors due to smoothing. Statistical errors on the image are found by inverting statistical errors on fluctuation data. The structure of this error distribution is usually simple, and can be characterized by a single number for each autocorrelation. Smoothing errors are estimated by passing inferred image \mathbf{I}_α a second time through the integration/inversion process to obtain $\mathbf{I}_{\alpha\alpha}$. Difference $\mathbf{I}_\alpha - \mathbf{I}_{\alpha\alpha}$ provides an upper limit on the smoothing distortion (some of the change includes further reduction of statistical error). A typical image-smoothing error distribution is shown in Fig. 4 (right panel). The per-bin systematic error on autocorrelation distributions is typically a few percent of maximum autocorrelation

values, somewhat larger peak errors lying within small regions corresponding to large image gradients.

Pythia p-p 200 GeV n correlations The Pythia-6.131 Monte Carlo [20] was used to provide a high-statistics sample of 200 GeV p-p collision events. Analysis of those data provides a demonstration of the precision possible with fluctuation inversion and a check on the algebraic system of this paper. We make a comparison between autocorrelations determined directly according to Eq. (6) and indirectly by fluctuation inversion according to Eq. (13). In Fig. 5 are charge-independent (left panel, like-sign + unlike-sign pair combinations) and charge-dependent (right panel, like-sign – unlike-sign pair combinations) pair-number autocorrelations on difference variables $(\eta_\Delta, \phi_\Delta)$ [2]. The autocorrelations were obtained by fluctuation inversion (upper panels) and directly from binned pair numbers (lower panels). Detailed comparison of the shapes of each pair of distributions indicates that fluctuation inversion is a very precise method of determining autocorrelations.

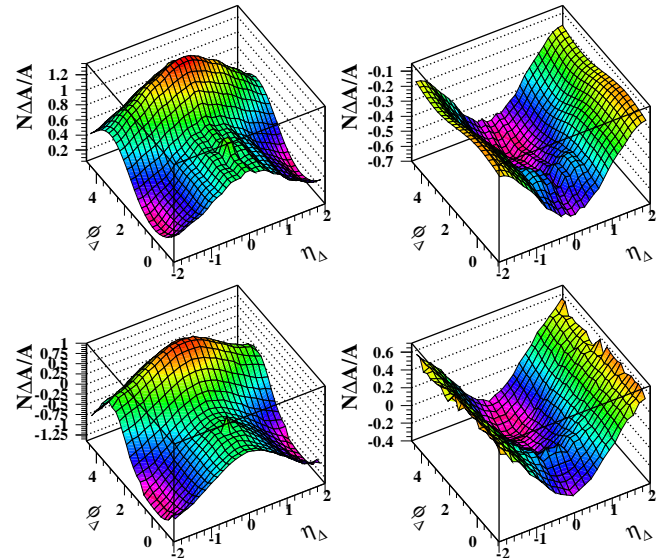


FIG. 5: Pair-number autocorrelations on difference variables $(\eta_\Delta, \phi_\Delta)$ for p-p collisions at 200 GeV from Pythia-6.131 obtained from fluctuation inversion (upper panels) and from direct pair counting (lower panels) for isoscalar (left panels) and isovector (right panels) autocorrelations.

The shift of vertical scale for upper and lower panels in Fig. 5 is due to the choice of sibling vs mixed pair normalization used in the direct determination of pair-number autocorrelations. Pair-number autocorrelations are constructed from pair sums $\hat{n}_{ij} \equiv n_{ij} / \sum_{ij} n_{ij}$ normalized to unit integral for sibling and mixed pairs [2]. Normalized pair-ratio histograms $\hat{r}_{ij} \equiv \hat{n}_{ij, obj} / \hat{n}_{ij, ref}$ are first formed on microbinned spaces (η_1, η_2) and (ϕ_1, ϕ_2) . Those distributions are then projected to form type-2 autocorrelation ratios $\Delta A_k^{(2)} / A_{k, ref} \equiv \hat{r}_k - 1$ on $(\eta_\Delta, \phi_\Delta)$. The pair-number difference autocorrelation $\Delta A_k^{(2)}$ so constructed

has zero integral, and therefore always varies about zero as in the lower panels of Fig. 5. Autocorrelations from fluctuation inversion retain their absolute vertical position: the offset missing from the zero-integral type-2 autocorrelation is equivalent to a fluctuation measurement at the acceptance scale. The factor \bar{N} in Fig. 5 defines a transitional form: $\bar{N}\Delta A_k^{(2)}/A_{k,ref} \simeq \Delta\eta\Delta\phi \cdot \Delta\rho/\sqrt{\rho_{ref}}$

IX. SUMMARY

Autocorrelation methods, broadly applied in science and engineering, provide a powerful means to study multiparticle correlations in nuclear collisions. Autocorrelations can be formed directly as pair ratios, which is however computationally intensive. Fluctuations are a related manifestation of multiparticle correlations which are easier to calculate but more difficult to interpret. If the correlation structure of a multiparticle distribution is approximately independent of absolute position in momentum space, the scale dependence of nonstatistical fluctuations can be inverted to obtain an autocorrelation distribution which represents nearly all of the two-particle correlation structure.

We have established in this paper the exact relation between correlations and fluctuations in the form of an integral equation. We have described the method required to invert that equation, and the procedure used to solve the technical problem of regularization of statistical noise. We have also described a procedure to determine statistical and systematic errors of the resulting autocorrelations, in particular distortions due to regularization. We have made detailed comparisons of autocorrelations determined directly from pair ratios and from fluctuation inversion with regularization which illustrate the precision of the method.

Autocorrelations obtained directly from pair ratios and by inversion from fluctuation scale dependence are complementary methods to access two-particle correlations. Pair ratios are most useful in low-multiplicity p-p and peripheral A-A collisions. Fluctuation inversion is essential for central A-A collisions. Detailed comparisons provide essential cross checks of the methods. For conditions common to nuclear collisions, fluctuations retain almost all correlation information. Inversion of fluctuation scale dependence recovers those correlations in a format that is directly interpretable.

-
- [1] E. A. De Wolf, I. M. Dremin and W. Kittel, Phys. Rept. **270**, 1 (1996), eprint hep-ph/9508325.
- [2] J. Adams *et al.* (STAR Collaboration), submitted to PRL, eprint nucl-ph/0406035.
- [3] E. V. Shuryak, Phys. Lett. **B 430** (1998) 9; M. Stephanov, K. Rajagopal, and E. Shuryak, Phys. Rev. Lett. **81** (1998) 4816.
- [4] M. Stephanov, K. Rajagopal, and E. Shuryak, Phys. Rev. **D 60** (1999) 114028.
- [5] B. Berdnikov and K. Rajagopal, Phys. Rev. **D 61** (2000) 105017; K. Rajagopal, Nucl. Phys. **A 680** (2000) 211.
- [6] R. Stock, Nucl. Phys. **A 661** (1999) 282.
- [7] G. Baym and H. Heiselberg, Phys. Lett. **B 469** (1999) 7;
- [8] T. A. Trainor, eprint hep-ph/0001148, unpublished.
- [9] J. Adams *et al.* (STAR Collaboration), eprint nucl-ex/0308033.
- [10] Kirsch, A, "An Introduction to the Mathematical Theory of Inverse Problems," Springer-Verlag, New York, 1996; Groetsch, C. W., "Inverse Problems in the Mathematical Sciences," Vieweg Publishing, Wiesbaden, 1993.
- [11] Box, G.E.P. and Jenkins, G. "Time series analysis: forecasting and control," Holden-Day (1976); Bendat, J.S. and Persol, A.G., "Random data — analysis and measurement procedures," 2nd Edition, John Wiley & Sons, NY (1986).
- [12] R. Brandelik *et al.*, Phys. Lett. **B100** 357 (1981); H. Aihara *et al.*, Phys. Rev. Lett. **53** 2199 (1984); P.D. Acton *et al.*, Phys. Lett. **B305** 415 (1993).
- [13] B. Andersson, Cambridge Monogr. Part. Phys. Nucl. Phys. Cosmol. **7**, 1 (1997).
- [14] J. Whitmore, Phys. Rept. **27**, 187 (1976); T. Kafka *et al.*, Phys. Rev. **D 16**, 1261 (1977).
- [15] U. A. Wiedemann and U. Heinz, Phys. Rep. **319**, 145 (1999).
- [16] H. C. Eggers, P. Lipa, P. Carruthers and B. Buschbeck, Phys. Rev. **D 48**, 2040 (1993); P. Lipa, P. Carruthers, H. C. Eggers and B. Buschbeck, Phys. Lett. **B 285**, 300 (1992).
- [17] Morozov, V. A. "Regularization Methods for Ill-Posed Problems," CRC Press, 1993; Engl, H. W., Hanke, M. and Neubauer, A., "Regularization of Inverse Problems," Kluwer, Dordrecht, 1996; Groetsch, C. W., "The Theory of Tikhonov Regularization for Fredholm Equations of the first Kind," Pitman, Boston, 1984; Corbard, T. *et al.*, astro-ph/9806359.
- [18] X. N. Wang and M. Gyulassy, Phys. Rev. **D 44**, 3501 (1991); M. Gyulassy and X.N. Wang, Comp. Phys. Comm. **83** (1994) 307.
- [19] Q.J. Liu, D.J. Prindle and T.A. Trainor, hep-ph/0410180.
- [20] T. Sjöstrand, Comput. Phys. Commun. **82**, 74 (1994); T. Sjöstrand, L. Lönnblad, S. Mrenna and P. Skands, eprint hep-ph/0308153.